

# Effects of physical parameter range on dimensionless variable sensitivity in water flooding reservoirs

Yu Hu Bai · Jia Chun Li · Ji Fu Zhou

Received: 8 October 2005 / Revised: 7 March 2006 / Published online: 24 May 2006  
© Springer-Verlag 2006

**Abstract** The similarity criterion for water flooding reservoir flows is concerned with in the present paper. When finding out all the dimensionless variables governing this kind of flow, their physical meanings are subsequently elucidated. Then, a numerical approach of sensitivity analysis is adopted to quantify their corresponding dominance degree among the similarity parameters. In this way, we may finally identify major scaling law in different parameter range and demonstrate the respective effects of viscosity, permeability and injection rate.

**Keywords** Physical parameter range · Dimensionless variable · Sensitivity analysis · Water flooding reservoir · Two-phase flow in porous media

## 1 Introduction

People have developed a number of recovery enhancement methods such as water, chemical, steam, carbon dioxide floodings, etc. when completing the primary stage of reservoir exploitation. In most circumstances, the mixing of injected and existing fluids in reservoir may result in a complex driving system. Numerous literatures have reported scaling laws of porous media flows in this kind of complex driving system for physical modeling. In regard to water flooding, Geertsma et al. [1]

derived similarity criteria for flows in cold and heated water flooding by using both inspection and dimension analysis. Kong et al. [2], Zhu et al. [3] and Shen et al. [4] made good supplements for the scaling criteria of water flooding. As for thermal exploitation, Stegemeier et al. [5] presented the scaling criteria for low pressure model, whereas Pujol and Beberg [6] did the same for high pressure model. Kimber et al. [7] obtained a set of scaling laws for steam and steam additive recovery reservoir for highly viscous oil. Similar studies were performed for steam flooding [8,9], electricity heating (Wang et al. [10,11]) and in-situ combustion [12,13] as well. Islam et al. [14] got the scaling criteria in polymer, emulsion and foam flooding experiments by the inspection. Islam et al. [15] gained the scaling criteria of surfactant-enhanced alkaline/polymer multiple flooding flows. Slavash et al. [16], Rojas et al. [17], Erdal et al. [18], Grattoni et al. [19] and Ekwere [20] dealt with the similarity law for CO<sub>2</sub> flooding reservoir.

Though numerous work has been reported on scaling law, few literatures have involved the dominance degree of scaling criteria quantitatively, which is important in physical modeling of reservoir. Generally speaking, there are a great many dimensionless variables representing the similarity of multi-phase flow in porous media with physical and chemical processes involved. Moreover, it is often very hard or sometimes even impossible to keep all of them in the laboratory experiment identical to the field test. For example, the precise scaling of both transverse dispersion and geometry may impractically require a huge model and an extremely long time interval in tests [21]. At the same time, modeling the ratios of the capillary and the driving forces to the gravitational force can induce a considerably high permeability, which can scarcely be realized in laboratory [4].

The project supported by the Innovative Project of CAS (KJCX-SW-L08) and the National Basic Research Program of China(973).

Y. H. Bai (✉) · J. C. Li · J. F. Zhou  
Division of Engineering Sciences, Institute of Mechanics,  
Chinese Academy of Sciences, Beijing 100080, China  
e-mail: byh\_2002@163.com

An efficient and practical way out is to single out the dominant variables and relax secondary ones in experiments. However, they very likely vary with physical parameter range. That is to say, the dominant variables for one reservoir may not be appropriate for another. Unfortunately, few literatures have coped with this issue thus far.

Based on the scaling criteria of water flooding reservoir, the authors have demonstrated the variation tendency of dominance degree for each dimensionless variable with physical parameter range in the following sections. To begin with, qualitative analysis of dimensionless variables is theoretically performed. The sensitivity factors are then calculated numerically in order to identify dominant and secondary ones in different physical parameter ranges. Finally, the effects of oil viscosity, permeability and injection rate are considered in more detail.

### 2 Similarity analysis

Let's consider the scaling criteria of a 3-D water flooding reservoir with the effects of the gravity, capillarity and compressibility of media involved. The dimensionless variables are found to be as follows [22,23]

$$\begin{aligned}
 \pi_1 &= \frac{K_{cwo}}{K_{row}}, \quad \pi_2 = \frac{K_o}{K_{cwo}}, \quad \pi_3 = \frac{K_w}{K_{row}}, \\
 \pi_4 &= \frac{y_R}{x_R}, \quad \pi_5 = \frac{x_R}{z_R}, \quad \pi_6 = \frac{x_p}{x_R}, \\
 \pi_7 &= \frac{y_p}{y_R}, \quad \pi_8 = \frac{r_{eo}}{x_R}, \quad \pi_9 = \frac{r_o}{x_R}, \\
 \pi_{10} &= \frac{s_{cw}}{\Delta s}, \quad \pi_{11} = \frac{s_{ro}}{\Delta s}, \quad \pi_{12} = \frac{s_{wi} - s_{cw}}{\Delta s}, \\
 \pi_{13} &= \frac{\sigma \sqrt{\frac{\phi_0}{K}} \cos \theta K_{row} h}{q_1 \mu_w}, \quad \pi_{14} = \frac{\mu_o}{\mu_w}, \quad \pi_{15} = \frac{\rho_{o0}}{\rho_{w0}}, \\
 \pi_{16} &= \frac{K_{row} h}{q_1 \mu_w} \rho_w g z_R, \quad \pi_{17} = \frac{C_o q_1 \mu_w}{K_{row} h}, \quad \pi_{18} = \frac{C_w q_1 \mu_w}{K_{row} h}, \\
 \pi_{19} &= \frac{C_\phi q_w \mu_w}{K_{row} h}, \quad \pi_{20} = \frac{p_{w0} K_{row} h}{q_1 \mu_w}, \quad \pi_{21} = \frac{p_{o0} K_{row} h}{q_1 \mu_w}, \\
 \pi_{22} &= \frac{p_{wf} K_{row} h}{q_1 \mu_w}, \quad \pi_{23} = \frac{p_{oi} K_{row} h}{q_1 \mu_w}, \quad \pi_{24} = J(\bar{s}_w), \quad (1)
 \end{aligned}$$

where  $p, \mu, \rho, K, \phi$  and  $s$  represent pressure, viscosity, density, effective permeability, porosity and saturation with subscripts w and o indicating water and oil phases, respectively.  $K_{cwo}$  refers to the effective permeability of oil phase under the condition of the irreducible water saturation,  $K_{row}$  that of water phase under the condition of the residual oil saturation,  $x_R, y_R$  and  $z_R$  reference length scale in three coordinate directions,

respectively,  $x_p$  and  $y_p$  the location of production well,  $r_o$  the well radius,  $s_{wi}$  the initial water saturation,  $\sigma$  and  $\theta$  the interfacial tension and contact angle between water and oil phases,  $g$  the gravitational acceleration,  $q_1$  the injection rate. The subscript 0 indicates physical quantities at a certain condition.  $C_o, C_w$  and  $C_\phi$  are the compressibility of oil, water and rock, respectively,  $p_{oi}$  the initial oil pressure and  $J(s_w)$  the capillary force function.  $\Delta s = 1 - s_{cw} - s_{ro}$  means the mobile oil saturation, in which  $s_{ro}$  and  $s_{cw}$  denote residual oil saturation and the irreducible water saturation, respectively.

From the physical point of view,  $\pi_1, \pi_2$  and  $\pi_3$  are the permeability similarity parameters,  $\pi_4, \pi_5, \pi_6, \pi_7, \pi_8$  and  $\pi_9$  the similarity in geometry,  $\pi_{10}$  and  $\pi_{11}$  the ratios of the irreducible water and residual oil saturation to the mobile oil saturation,  $\pi_{12}$  the reduced initial water saturation,  $\pi_{14}$  and  $\pi_{15}$  the ratios of the viscosity and density of water to oil,  $\pi_{13}$  and  $\pi_{16}$  the ratios of the capillary and gravity forces to the driving force,  $\pi_{17}, \pi_{18}$  and  $\pi_{19}$  the relative volume variation ratios of oil, water and rock under the reservoir pressure, respectively.  $\pi_{20}, \pi_{21}, \pi_{22}$  and  $\pi_{23}$  denote the respective ratios of the reference pressure of oil and water, the bottom pressure of the production well, and the initial pressure to the reservoir pressure difference.  $\pi_{24}$  is the dimensionless capillary force function. More specifically, we may make analysis in more detail as follows.

$\pi_{11}$  can be apparently put in the following form

$$\frac{s_{ro} \phi}{(1 - s_{cw} - s_{ro}) \phi}, \quad (2)$$

where the numerator and the denominator mean the volume portions of the residual and mobile oil. Therefore,  $\pi_{11}$  denotes the volume ratio between the residual and mobile oil. Similarly,  $\pi_{10}$  is the volume ratio between the irreducible water and mobile oil.

$\pi_{13}$  can be rewritten as

$$\frac{\sigma / \sqrt{K / \phi_0}}{q_1 \mu_w / (K_{row} h)}, \quad (3)$$

where  $\sqrt{K / \phi_0}$  is the average pore radius and hence  $\sigma / \sqrt{K / \phi_0}$  turns out the capillary force in the same pore. The denominator is equivalent to the pressure difference needed to keep the injection rate  $q_1$  in the reservoir, i. e.

$$\frac{q_1 \mu_w}{K_{row} h} \sim \Delta p. \quad (4)$$

Consequently,  $\pi_{13}$  implies the relative importance between capillary force and displacement pressure. In most situations, capillary force is far less than displacement pressure and so  $\pi_{13}$  is secondary. However, if the permeability is high or the injection rate is small enough,

the capillary force may become comparable to or even exceed driving pressure. In this case,  $\pi_{13}$  cannot be assumed negligible any more.

$\pi_{14}$  plays an important role to maintain stability between oil and water interface in the process of displacement, thus directly affecting sweeping efficiency. When the interface becomes unstable in a certain range of  $\pi_{14}$ , fingering phenomenon occurs, thus leads to the diminution of sweeping area and efficiency. On the contrary, the stable displacement can enhance efficiency.

$\pi_{16}$  is obviously equivalent to  $\rho_{w0}gz_R/\Delta p$ , which signifies the ratio of the static and dynamic pressure. In a thinner reservoir or under higher injection rate, the flow is mainly governed by the driving force. As reservoir thickness grows or the injection rate drops, the effect of the gravity becomes more evident such that  $\pi_{16}$  turns to dominant.

$\pi_{17}$ ,  $\pi_{18}$  and  $\pi_{19}$  can be rewritten in the same form

$$\frac{C_l q_l \mu_w}{K_{row} h} = C_l \Delta p, \quad l = o, w, \phi. \tag{5}$$

With the growth of the injection rate or underground pressure, the relative volume variation of water, oil and rock media magnifies and then  $\pi_{17}$ ,  $\pi_{18}$ ,  $\pi_{19}$  become significant.

The variation tendency of the dominance degree of  $\pi_{22}$  with physical parameter range can be clarified in the same way:

$$\frac{p_{wf} K_{row} h}{q_l \mu_w} \sim \frac{p_{wf}}{\Delta p} \sim \frac{1}{p_{inj}/p_{wf} - 1}, \tag{6}$$

which reflects the relative importance of the injection pressure  $p_{inj}$  and the well bottom pressure  $p_{wf}$ .  $\pi_{22}$  becomes significant with increasing injection pressure or decreasing production pressure.

Up to now, we can see that the dominance degree of each dimensionless variable is not always invariant within the physical parameter range. Therefore, numerical approach is applied to display this kind of variation quantitatively instead of qualitatively as previously stated.

### 3 Numerical approach to analyze the sensitivity of dimensionless variables

Based on sensitivity analysis proposed in our previous work [23], the variation tendency of the dominance degree of dimensionless variables in different physical parameter range is investigated numerically. The sensitivity factor of the dimensionless variable  $\pi_i$  can be defined as

$$S_i = \frac{\partial [f(\pi_1, \pi_2, \dots, \pi_N)/f_p]}{\partial (\pi_i/\pi_{ip})}, \quad i = 1, 2, \dots, N, \tag{7}$$

where  $f(\pi_1, \pi_2, \dots, \pi_N)$  is a target function concerned in the experiment. The subscript  $p$  represents the prototype. In a water flooding experiment, the target function can be selected as oil recovery, which looks like

$$f(\pi_1, \pi_2, \dots, \pi_N) = \int_0^{T_D} \eta(\pi_1, \pi_2, \dots, \pi_N, t_D) dt_D, \tag{8}$$

where  $\eta(\pi_1, \pi_2, \dots, \pi_N, t_D)$  represents the oil recovery curve,  $T_D$  the dimensionless time span of development. Then, the sensitivity factor is calculated according to

$$S_i = \frac{\int_0^{T_D} |\eta_m - \eta_p| dt_D / \int_0^{T_D} \eta_p dt_D}{|(\pi_{im} - \pi_{ip})/\pi_{ip}|}, \tag{9}$$

where the subscript m represents the model. For a given set of physical parameters, the relative variation of the target function with respect to a specific dimensionless variable is calculated and the sensitivity factors are determined in this way. Comparing the sensitivity factors in different physical parameter range, we may yield the variation tendency of the dominance degree for each dimensionless parameter.

As usual, the dimensionless governing equations of porous media flows during water flooding can be written as

$$\begin{aligned} & \pi_1 \pi_4 \frac{\partial}{\partial x_D} \left( \rho_{oD} \frac{K_{oD}}{\mu_{oD}} \frac{\partial p_{oD}}{\partial x_D} \right) + \frac{\pi_1}{\pi_4} \frac{\partial}{\partial y_D} \left( \rho_{oD} \frac{K_{oD}}{\mu_{oD}} \frac{\partial p_{oD}}{\partial y_D} \right) \\ & + \pi_1 \pi_4 \pi_5^2 \frac{\partial}{\partial z_D} \left( \rho_{oD} \frac{K_{oD}}{\mu_{oD}} \frac{\partial p_{oD}}{\partial z_D} \right) \\ & + \pi_{16} \pi_1 \pi_4 \pi_5^2 \frac{\partial}{\partial z_D} \left( \rho_{oD}^2 \rho_{o0D} \frac{K_{oD}}{\mu_{oD}} \right) \\ & + \pi_1 \rho_{oD} \frac{\pi K_{oD} (p_{wfD} - p_{oD})}{2 \ln r_{eOD}/r_{oD}} \delta(x_D - \pi_6) \delta(y_D - \pi_7) \\ & = \frac{\partial(\phi_D \rho_{oD} \bar{s}_o)}{\partial t_D} + \pi_{11} \frac{\partial(\rho_{oD} \phi_{oD})}{\partial t_D}, \tag{10} \\ & \pi_4 \frac{\partial}{\partial x_D} \left( \rho_{wD} K_{wD} \frac{\partial p_{wD}}{\partial x_D} \right) + \frac{1}{\pi_4} \frac{\partial}{\partial y_D} \left( \rho_{wD} K_{wD} \frac{\partial p_{wD}}{\partial y_D} \right) \\ & + \pi_4 \pi_5^2 \frac{\partial}{\partial z_D} \left( \rho_{wD} K_{wD} \frac{\partial p_{wD}}{\partial z_D} \right) + \pi_{16} \pi_4 \pi_5^2 \frac{\partial}{\partial z_D} (\rho_{wD}^2 K_{wD}) \\ & + \rho_{wD} \left[ \frac{1}{4} \delta(x_D) \delta(y_D) + \frac{\pi K_{wD} (p_{wfD} - p_{wD})}{2 \ln r_{eOD}/r_{oD}} \right. \\ & \left. \times \delta(x_D - \pi_6) \delta(y_D - \pi_7) \right] = \frac{\partial(\phi_D \rho_{wD} \bar{s}_w)}{\partial t_D} + \pi_{10} \frac{\partial(\rho_{wD} \phi_D)}{\partial t_D}. \tag{11} \end{aligned}$$

The dimensionless capillary force equation is put in the form

$$p_{cD} = (p_{oD} - p_{wD}) = \pi_{13} \sqrt{\phi_D} J(\bar{s}_w), \tag{12}$$

**Table 1** Major physical parameters

Parameters	$L$	$W$	$\sigma$	$q_1$	$k_{row}$	$k_{cwo}$
Prototype	140	140	2.50	8	0.37	0.78
Parameters	$\rho_o$	$\rho_w$	$\mu_o$	$C_\phi$	$p_{w0}$	$p_{o0}$
	$/(kg \cdot m^{-3})$	$/(kg \cdot m^{-3})$	$\times 10^{-3}/(Pa \cdot s)$	$\times 10^{-10}/Pa^{-1}$	$\times 10^6/Pa$	$\times 10^6/Pa$
Prototype	800	1 000	5	6.0	12.0	12.0
Parameters	$h$	$g$	$C_o$	$C_w$	$p_{wf}$	$p_{oi}$
	$/m$	$/(m \cdot s^{-2})$	$\times 10^{-10}/Pa^{-1}$	$\times 10^{-10}/Pa^{-1}$	$\times 10^6/Pa$	$\times 10^6/Pa$
Prototype	10	9.8	8.0	5.0	10.0	12.0

with dimensionless saturation relation

$$\bar{s}_o + \bar{s}_w = 1. \tag{13}$$

The dimensionless initial conditions are specified by

$$p_{oD}|_{t_D=0} = p_{oiD}, \quad \bar{s}_w|_{t=0} = \bar{s}_{wi}, \tag{14}$$

and the corresponding boundary conditions are

$$\begin{aligned} \frac{\partial p_{lD}}{\partial x_D} = 0, \quad \frac{\partial p_{lD}}{\partial y_D} = 0, \\ \frac{\partial p_{lD}}{\partial z_D} + \pi_{16} \rho_{lD} = 0, \quad l = o, w \end{aligned} \tag{15}$$

where

$$\begin{aligned} \rho_{wD} &= 1 + C_{wD}(p_{wD} - p_{w0D}) + \pi_{16} C_{wD} z_D, \\ \rho_{oD} &= 1 + C_{oD}(p_{oD} - p_{o0D}) + \pi_{16} C_{oD} \rho_{o0D} z_D, \\ \phi_D &= 1 + C_{\phi D} \left( \frac{p_{wD} + p_{oD}}{2} - \frac{p_{w0D} + p_{o0D}}{2} \right) \\ &\quad + \frac{\pi_{16}}{2} (\rho_{o0D} C_{\phi D} z_D + C_{\phi D} z_D). \end{aligned}$$

In the above equations, the subscript D denotes dimensionless variable. The governing equations are discretized using finite difference scheme and solved by the conventional implicit pressure-explicit saturation method (IMPES) [23,24]. The main physical parameters are listed in Table 1.

### 4 Results and discussion

Based on previous numerical sensitivity analysis, the variation tendency of the dominance degree of dimensionless variables with physical parameter range such as oil viscosity, permeability and injection rate is shown in the following in turn.

#### 4.1 Oil viscosity effect

Water flooding reservoirs usually can be classified as low ( $\mu_o < 3 \text{ mPa} \cdot \text{s}$ ), moderate ( $3 < \mu_o < 30 \text{ mPa} \cdot \text{s}$ ) and high viscosity ( $\mu_o > 30 \text{ mPa} \cdot \text{s}$ ) [25]. Assuming  $\mu_o$  equal to 2.5, 5 and 50  $\text{mPa} \cdot \text{s}$ , respectively, and keeping

the other parameters unchanged, the sensitivity factors for water flooding reservoir with low, moderate and high viscosity can be calculated as shown in Fig. 1. A line of 0.1 demarcating the sensitivity factor level of the dominant and secondary dimensionless variables is also given in the same diagram. That is to say, the dimensionless variable is regarded as a dominant one if its sensitivity factor is greater than 0.1. Otherwise, it is deemed as a secondary one. This rule also applies in the following texts. It is obviously seen from Fig. 1 that the sensitivity factors, indicating the dominance degree of each dimensionless variable, change with oil viscosity. In particular, the dominant dimensionless variables are different for reservoirs with different oil viscosity. Namely, they are  $\pi_1, \pi_2, \pi_3, \pi_{12}, \pi_{14}$  and  $\pi_{15}$  for low and moderate oil viscosity reservoirs and  $\pi_1, \pi_2, \pi_3, \pi_{10}, \pi_{12}$  and  $\pi_{14}$  for high oil viscosity reservoir.

Obviously,  $\pi_{10}$  turns from a secondary dimensionless variable for low and moderate viscosity reservoirs to a dominant one for high viscosity reservoir. This is simply because high viscosity reduces oil recovery and total exploited oil volume. Hence,  $\pi_{10}$  representing the ratio of irreducible water and mobile oil become significant and may dramatically affect the final oil recovery. On the contrary, the high oil recovery in low viscosity reservoir has larger amount of total exploited oil volume, meaning that the irreducible water can be neglected.

Also we may notice that the dimensionless variable  $\pi_{15}$  turns from a dominant one in the low and moderate viscosity reservoirs to a secondary one in high viscosity reservoir. As mentioned above,  $\pi_{15}$  represents the density ratio of the oil to water phases, and also can be explained as the inertial force ratio. As oil viscosity increases, the driving force needed increases tremendously with almost unchanged density ratio. Therefore, the driving pressure to overcome viscosity exerts more influence on the reservoir flows than the inertial force does. The effect of density on the oil recovery is weakened as oil viscosity rises.

The sensitivity factors of  $\pi_{17}, \pi_{18}$  and  $\pi_{19}$  may increase with oil viscosity by almost two-order of magnitude. The reason of which is that to overcome viscous resistance,

**Fig. 1** The effect of the variation of oil viscosity on the dominance degree where *white, gray and black* indicate low, moderate and high oil viscosity, respectively

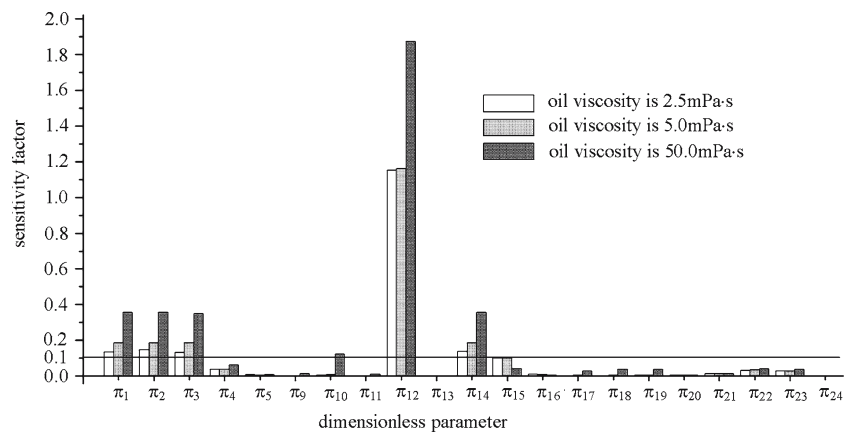
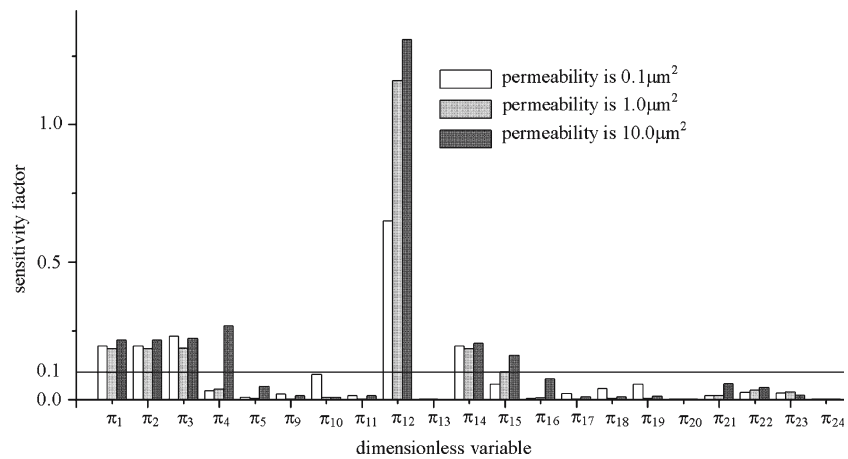


**Fig. 2** The effect of the variation of permeability on the dominance degree where *white, gray and black* indicate low, moderate and high permeability, respectively



the augment of the driving pressure causes relatively large volume variation in water, oil and rock.

### 4.2 Permeability effect

We presumably choose 0.1, 1 and 10 Darcy as low, moderate and high permeability to study the effect of permeability on the dominance degree of dimensionless variables. We can see in Fig. 2 that the dominant variables are  $\pi_1, \pi_2, \pi_3, \pi_{10}, \pi_{12}$  and  $\pi_{14}$  in low permeability reservoir,  $\pi_1, \pi_2, \pi_3, \pi_{12}, \pi_{14}$  and  $\pi_{15}$  in moderate permeability reservoir, and  $\pi_1, \pi_2, \pi_3, \pi_4, \pi_{12}, \pi_{14}$  and  $\pi_{15}$  in high permeability reservoir.

$\pi_4$  becomes a dominant one in high permeability case. As we know, the sweeping area increases with the permeability. Therefore, whether the geometry is similar or not exerts an evident effect on the oil recovery. The larger the permeability, the more important the geometric similarity.

$\pi_{10}$  turns close to a dominant variable from a secondary one with the decreasing of permeability. For low permeability case, the resistance to flow grows and results in the decrease of oil recovery and total exploited oil volume. Therefore, the variation of the irreducible

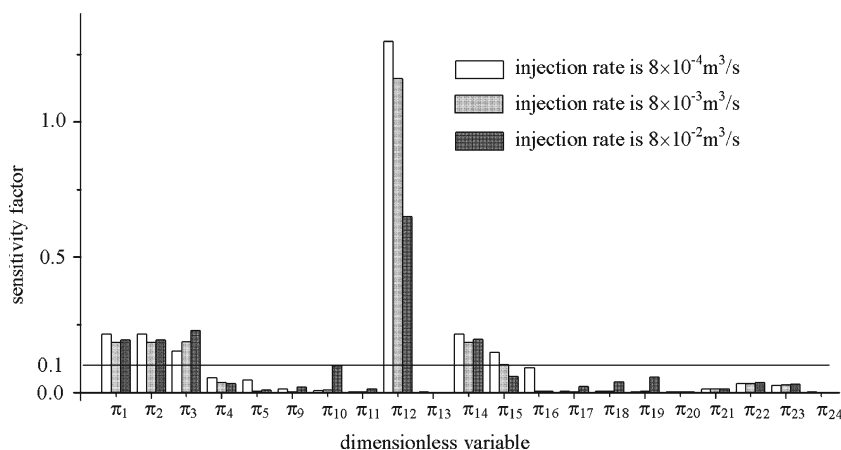
water volume exerts evident influences on the final oil recovery.

$\pi_{15}$  turns from a dominant variable in the moderate and high permeability cases to a secondary one in the low permeability reservoir. This is because the augmentation of the pressure difference in the lower permeability reservoir may weaken the effect of the inertial force. The sensitivity of  $\pi_{16}$  increases with permeability. The higher the permeability, the smaller the driving force and the role of gravity becomes more evident. In addition, we should pay particular attention to  $\pi_{17}, \pi_{18}$  and  $\pi_{19}$  in low permeability reservoirs when the driving force, namely the pressure difference, is increasing. The situation definitely implies that we should consider the compressibility effect of water, oil and rock.

### 4.3 Injection rate effect

To fit for different rock characteristics or exploitation requirement, the injection rate may be adjusted time and again. Then, new balance among all kinds of forces is reestablished with of the driving pressure in oil reservoir. Selecting  $8 \times 10^{-4}, 8 \times 10^{-3}$  and  $8 \times 10^{-2} \text{ m}^3/\text{s}$  as low, moderate and high injection rates, we explore the variation tendency of the sensitivity factors of all

**Fig. 3** The effect of the variation of injection rate on dominance degree where *white, gray* and *black* indicate low, moderate and high injection rate cases, respectively



dimensionless variables with injection rate. The results are plotted in Fig. 3, showing that  $\pi_1, \pi_2, \pi_3, \pi_{12}, \pi_{14}, \pi_{15}, \pi_{16}$  are the dominant variables for low injection rates, and  $\pi_1, \pi_2, \pi_3, \pi_{12}, \pi_{14}, \pi_{15}$  and  $\pi_1, \pi_2, \pi_3, \pi_{10}, \pi_{12}, \pi_{14}$  for moderate and high injection rates, respectively.

The sensitivity of  $\pi_{16}$  representing the relative importance between the gravity and driving force, increases with the drop of injection rate. Apparently, the effects of the gravity cannot be neglected for low injection rate case with smaller driving force.

$\pi_{10}$  is dominant at high injection rate. To some extent, oil recovery increases with the injection rate. However, this is not always true. Very high injection rate may cause early happening of water break-through and flooding out, which reduces oil recovery and total exploited oil volume. The fact once again accounts for the dominance of  $\pi_{10}$  at high injection rate as stated in Sect. 4.1 and 4.2.

With the increasing of the injection rate,  $\pi_{15}$ , the density ratio may become secondary from a dominant one. The reason is that at high injection rate, namely high driving force, the inertial force exerts less effect on reservoir flow than the driving force.

Once again, we find out that the sensitivity factors of  $\pi_{17}, \pi_{18}$  and  $\pi_{19}$  increase with the injection rate. Since the pressure difference is proportional to injection rate, water, oil and rock can no longer be regarded as incompressible in high pressure environment. The compressibility or the volume variation of water, oil and rock should be taken into consideration.

## 5 Concluding remarks

As we know, efficient technical measures taken for the enhancement of oil recovery are heavily dependent on the understanding of oil, water and polymer seepage flows in the reservoir. Physical modeling has become an additional powerful tool as new apparatus of visual-

ization such as PIV, CT, NMR etc. appear. As a result, the study of similarity law of multiphase flows in porous media is put on agenda.

The present study in previous sections shows that all the similarity variables actually possess a definite physical meaning. Namely, they indeed imply some kinds of ratios of geometric scales, or of medium properties, or of driving forces, which obviously vary with the range of physical parameters. In the present article, we have examined the effects of most significant factors in practical petroleum engineering such as viscosity, permeability and injection rate. For highly viscous or low permeability oil reservoir or under high injection rate condition, displacement pressure may be larger than other external forces such as capillary and gravitational forces, thus leading to some relevant similarity variables negligible. In contrast, rock deformation and liquid compressibility can not be neglected any more now and a model accounting for fluid-solid interaction should be given priority to. Furthermore, high viscosity, low permeability and high injection rate always mean or are equivalent to low oil recovery. That is to say, the amount of residual oil and irreducible water may occupy a significant portion of total exploited oil volume. Then the dimensionless variables indicating rock wettability of oil and water should be taken into consideration. The contrary argument can be drawn for low viscous and high permeability oil reservoir and under low injection rate conditions. The above conclusions may serve as a guideline in the physical modeling for water flooding oil reservoir, thus finding out dominant dimensionless variables. Generally speaking, the present numerical sensitivity methods may also be used in the study of other complicated physical problems in order to identify major similarity parameters.

Please notice that the present analysis needs revision if the fluid becomes non-Newtonian for high viscous reservoir or startup pressure is comparable to other

driving forces under low permeability condition. Probably, additional similarity parameters may play important roles in these circumstances.

## References

- Geertsma, J., Croes, G.A., Schwart, N.: Theory of dimensionally scaled model of petroleum reservoir. *Trans. AIME*, **207**, 118–127 (1956)
- Kong, X.Y., Chen, F.L.: Similarity criteria and physical simulation for water flooding (in Chinese). *Petroleum Explor. Dev* **24**(6), 56–60 (1997)
- Zhu, Z.H.: The feasibility of scaling the water flooding experiments with low pressure physical model (in Chinese). *Xinjiang Petroleum Sci. Technol.* **7**(2), 16–22 (1997)
- Shen, P.P.: *The Theory and Experiment of Water and Oil Flow in Porous Media* (in Chinese). Oil Industry Press Beijing (2000)
- Stegemeier, G.L., Volek, C.W., Laumbach, D.D.: Representing steam processes with vacuum models. *SPE* **6787**, 1977
- Pujol, L., Boberg, T.C.: Scaling accuracy of laboratory steam-flooding models. *SPE* **4191** (1972)
- Kimber, K.D., Farouq Ali, S.M., Puttagunta, V.R.: New scaling criteria and their talkative merits for steam recovery experiments. *J. Can. Petroleum Technol.* **27**(4), 86–94 (1988)
- Wang, L.Q., Zhou, H.Z.: Determination of parameters for the scaling reservoir physical model (in Chinese). *J. Tsinghua Univ. (Sci. Tech.)* **35**(2), 100–105 (1995)
- Chen, Y.Z., Guan, W.L.: Experiment of changing injection-production pattern with low pressure scaled physical model of steam drive production (in Chinese). *Spec. Oil Gas Reservoirs* **3**(2), 51–55 (1996)
- Wang, D.S., Guan, J.P., Wang, Y.D.: Study on electrical heating technique with the resistance for single well (in Chinese). *J. Univ. Petroleum (Sci. Tech.)* **22**(4), 54–58 (1998)
- Wang, D.S., Chen, Y.M., Guan, J.P.: Research on physical simulation of electrical heating reservoir (in Chinese). *J. Univ. Petroleum (Sci. Tech.)*, **25**(2), 54–58 (2001)
- Binder, G.G.: Scaled model tests of in-situ combustion in massive unconsolidated sands. In: *Proc. Seventh World Pet. Cong.*, Mexico City, pp 477–485 (1967)
- Garon, A.M., Geisbrecht, R.A., Lowry, W.E.: Scaled model experiments of fire flooding in tar sands. *SPE* **9449**, pp 2158–2166 (1982)
- Islam, M.R., Farouq Ali, S.M.: New scaling criteria for polymer emulsion and foam flooding experiments. *J. Can. Petroleum Technol.* **28**(4), 79–97 (1989)
- Islam, M.R., Farouq Ali, S.M.: New scaling criteria for chemical flooding experiments. *J. Can. Petroleum Technol.* **29**(1), 29–36 (1990)
- Slavash Gharib, Todd, M.D.: Physically scaled model simulating the displacement of residual oil by miscible CO<sub>2</sub> in linear geometry. *Soc. Petroleum Eng. AIME, SPE* **8896**, 1–10 (1980)
- Rojas, G., Farouq Ali, S.M.: Dynamics of subcritical carbon dioxide/brine floods for heavy oil recovery. *SPE* **13598**, 81–88 (1988)
- Erdal Tuzunoglu, Suat Bagci.: Scaled 3-D model studies of immiscible carbon dioxide flooding using horizontal wells. *J. Petroleum Sci. Eng.* **26**, 67–81 (2000)
- Grattoni, C.A., Jing, X.D., Dawe, R.A.: Dimensionless groups for three-phase gravity drainage flow in porous media. *J. Petroleum Sci. Eng.* **29**(1) 53–65 (2001)
- Ekwere, J.P.: Scaling unstable immiscible displacements. *SPE* **12331**, 1–6 (1983)
- Pozzi, A.L., Blackwell, R.J.: Design of laboratory models for study of miscible displacement. *SPE* **4**, 28–40 (1963)
- Bai, Y.H., Zhou, J.F., Li, J.C.: Numerical sensitivity analysis and partial similarity of porous media flows. In: *Proceeding of the Fourth International Conference on Fluid Mechanics*, Dalian, 2004-07-21-24, pp 397–402 (2004)
- Bai, Y.H., Li, J.C., Zhou, J.F.: Sensitivity analysis of dimensionless parameters for physical simulation of water flooding reservoir. *Sci. China Series E* **48**(4), 441–453 (2005)
- Khalid Aziz, Antonin Settari. *Petroleum Reservoir Simulation*. Applied Science Publishers, New York (1979)
- Yu, Q.T.: A new method to forecast the raising of water content in water flooding sand reservoir (in Chinese). *Xinjiang Petroleum Geol* **23**(4), 314–316 (2002)